Mechanics Research Communications 140 (2024) 104321

Contents lists available at ScienceDirect

Mechanics Research Communications

journal homepage: www.elsevier.com/locate/mechrescom

Flexoelectric anisotropy and shear contributions in lead-free piezocomposites

A.K. Jagdish [a], Federico C. Buroni [b,*], Roderick Melnik [a,b], Luis Rodriguez-Tembleque [c], Andrés Sáez [c]

[a] MS2Discovery Interdisciplinary Research Institute, Wilfrid Laurier University, 75 University Ave W, Waterloo, Ontario, N2L 3C5, Canada
[b] Department of Mechanical Engineering and Manufacturing, Universidad de Sevilla, Camino de los Descubrimientos s/n, Seville E-41092, Spain
[c] Department of Continuum Mechanics and Structural Analysis, Universidad de Sevilla, Camino de los Descubrimientos s/n, Seville E-41092, Spain

ARTICLE INFO

Keywords:
Shear flexoelectricity
Textured flexoelectricity
Auxetic matrix
Incompressible matrix
Flexoelectric coefficients

ABSTRACT

Flexoelectricity is the coupling between strain gradients and electric fields. This phenomenon can significantly enhance piezocomposite response in addition to linear piezoelectricity. This enhancement is especially important for lead-free piezocomposites, which generally underperform compared to lead-based counterparts. Flexoelectric enhancement is facilitated by structural anisotropy in piezocomposites. However, challenges in modeling flexoelectric effects arise from several unknowns. Firstly, the shear flexoelectric coefficient is not well-characterized experimentally. Secondly, significant discrepancies exist between theoretical predictions and experimental measurements of flexoelectric coefficients. Thirdly, the influence of matrix mechanical properties on flexoelectric behavior is poorly understood. To address these issues, we construct a parametric flexoelectric model of a lead-free piezocomposite with graded inclusion concentration. We then systematically analyze the impact of each parameter to identify which significantly influence flexoelectric behavior. This study is intended to provide direction to further experimental studies towards understanding and tailoring this subset of parameters.

1. Introduction

Flexoelectricity is the coupling between strain gradients and electric fields [1,2]. Unlike piezoelectricity, which is a coupling between strain and electric fields, flexoelectric coupling can occur even in materials with inversion symmetry. Harnessing this coupled process can widen the gamut of commonly available materials that can be used for many interesting electromechanical applications. Strain gradients can be brought about in otherwise homogeneous materials by inducing anisotropy in structure and electromechanical properties. This direction has been explored both in the context of bulk materials [3,4] and, more recently, flexoelectric composites [5-7]. These studies have shown that flexoelectricity holds promise in enhancing electromechanical performance in the contexts of sensing, actuating, and energy generation. These alternative modes of enhancing electromechanical coupling are key in boosting the efficiencies of lead-free piezoelectric materials, such as $BaTiO_3$, particularly given their inferior performance compared to lead-based piezoelectric materials [8,9]. Further, flexoelectricity plays a key role in polarization coupling across ferroelectric domains in polycrystalline piezoelectric materials [10]. This is particularly an important effect to properly understand to accurately model flexoelectric composites based on low-cost polycrystalline, environmentally friendly, lead-free materials such as $BaTiO_3$. However, the accurate design of flexoelectric materials, particularly composites, faces significant challenges due to several variables. These include, primarily, the mismatch between the experimentally measured and theoretically predicted values of the transverse and longitudinal flexoelectric coefficients [11], which is around three orders of magnitude. Secondly, the shear flexoelectric coefficient is not well-characterized and does not have well-defined values in the literature [12]. Further, this gap in the understanding and the importance of filling it has been pointed out in the literature [10,13]. Thirdly, the matrix in which flexoelectric inclusions are dispersed plays an important role in determining the flexoelectric behaviour of the composite. However, the role of several matrix properties in influencing flexoelectricity, particularly the Poisson's ratio, has not been explored. Hence, we aim to better understand the influence of

* Corresponding author.
E-mail address: fburoni@us.es (F.C. Buroni).

https://doi.org/10.1016/j.mechrescom.2024.104321
Received 24 July 2024; Received in revised form 13 August 2024; Accepted 21 August 2024
Available online 30 August 2024

these factors by constructing and analyzing a parametric coupled flexoelectric model for a lead-free piezocomposite based on $BaTiO_3$ inclusions. This study is particularly important to lead-free composites given their inferior piezoelectric performance compared to lead-based materials, which can be enhanced by flexoelectric optimization. The objective of the study is to identify the factors that most significantly influence flexoelectric coupling so that appropriate experimental studies can be conducted towards better characterizing these factors. A further objective is also to provide direction towards optimized engineering of electromechanical composites to enhance flexoelectric performance by maximizing the factors that have considerable influence on flexoelectric properties of the composite.

2. Modelling framework to evaluate flexoelectric contributions

In this section, we first develop the fully coupled electro-elastic model combining linear piezoelectricity, flexoelectricity, and electrostriction. We further discuss the RVE (Representative Volume Element) geometry adopted for the study and the corresponding boundary conditions used for the finite element analysis.

2.1. Generalized coupled electro-mechanical model

We start with the Gibbs free energy function that includes linear piezoelectric, flexoelectric, and electrostrictive coupling. This is given by [5,12,14-16]:

$$G = \frac{1}{2}c_{ijkl}\varepsilon_{ij}\varepsilon_{kl} - \frac{1}{2}\epsilon_{ij}E_iE_j - e_{kij}E_k\varepsilon_{ij} - \frac{1}{2}B_{klij}E_kE_l\varepsilon_{ij} - \mu_{ijkl}E_i\varepsilon_{jk,l}, \tag{1}$$

where c_{ijkl}, ε_{ij}, e_{ijk}, B_{ijkl}, and μ_{ijkl} are the elastic coefficients, the permittivity, the piezoelectric, electrostrictive, and flexoelectric coefficients, respectively. The variables ε_{ij}, E_i, and $\varepsilon_{jk,l}$ represent the components of the strain tensor, electric field components, and strain-gradient fields. This model is a generalization of the linear piezoelectric model which is described by the free energy function, excluding flexoelectric and nonlinear couplings, would be $G = \frac{1}{2}c_{ijkl}\varepsilon_{ij}\varepsilon_{kl} - \frac{1}{2}\epsilon_{ij}E_iE_j - e_{kij}E_k\varepsilon_{ij}$ [17-19]. Although size-dependent elasticity is another coupling that ideally needs to be included in the model [20-23], we have neglected it in Eq. (1). This is because size-dependent elasticity operates mainly at size scales of 1–10 nm [24] whereas our analysis considers size scales that are at least an order of magnitude larger.

From Eq. (1), the following phenomenological relations to determine the electro-elastic behaviour of the flexoelectric composites are derived:

$$\sigma_{ij} = \frac{\partial G}{\partial \varepsilon_{ij}} = c_{ijkl}\varepsilon_{kl} - e_{kij}E_k - \frac{1}{2}B_{klij}E_kE_l, \tag{2}$$

$$\widehat{\sigma}_{ijk} = \frac{\partial G}{\partial \varepsilon_{ij,k}} = -\mu_{lijk}E_l, \tag{3}$$

$$D_i = -\frac{\partial G}{\partial E_i} = \epsilon_{ij}E_j + e_{ijk}\varepsilon_{jk} + B_{ijkl}E_j\varepsilon_{kl} + \mu_{ijkl}\varepsilon_{jk,l}. \tag{4}$$

Here, σ_{ij} standard stress tensor components, $\widehat{\sigma}_{ijk}$ represents the higher order stress tensor components, and D_i represents the electric flux density components. The balance equations governing the above relations are [6,25]:

$$\left(\sigma_{ij} - \widehat{\sigma}_{ijk,k}\right)_{,j} + F_i = 0, \tag{5}$$

$$D_{i,i} = 0, \tag{6}$$

where F_i are the body force components assumed to vanish in the set of computational experiments presented in Section 3.

Further, the Cauchy relationship is used to express the strain components as $\varepsilon_{ij} = \frac{1}{2}\left(u_{i,j} + u_{j,i}\right)$ - in terms of the derivatives of the displacements. The electric field is related to the electric potential by $E_i = -V_{,i}$. Using these relationships and by substituting Eqs. (2)-(4) in Eqs. (5) and (6), we obtain a system of nonlinear, nonlocal differential equations in u_i and V. The model is implemented in finite element method using COMSOL Multiphysics software.

2.2. RVE geometry and boundary conditions

For our study, we chose a two-dimensional rectangular RVE with sides a_m and b_m(Fig. 1(a)). We consider a graded inclusion concentration, as shown in the figure. We use randomly shaped inclusions that are spatially constrained within radii R_1 and R_2 ($R_2 > R_1$). We scale the length scales along both the x and y axes by a scaling factor $N$to study the size-dependent flexoelectric effects. When $N = 1$, the RVE dimensions are $a_m = b_m = 50\mu m$. R_1 and R_2 have been picked randomly within the ranges [2.5–3.5 μm] and [4.0–5.0 μm], respectively, for each point defined by the random polygonal structure of the inclusion.

Figure 1(b)-(c) show the boundary conditions BC1 and BC2, respectively, that are used in this study to obtain the effective piezoelectric coefficients e_{31} and e_{33}, respectively [6,25]. We, further, use Lagrange quadratic shape functions for the dependent variables u_1,u_2 and V because it is seen that second order functions typically better represent the physical model in flexoelectric simulations [26]. The effective piezoelectric coefficients $e_{31}$and e_{33} are calculated as follows [27,28]:

$$e_{31} = \frac{D_3}{\overline{\varepsilon}_{11}}, \quad e_{33} = \frac{D_3}{\overline{\varepsilon}_{33}}, \tag{7}$$

where Xrepresents the volume average of the variable X.

2.3. Material properties

The materials making up the composite are the matrix and the piezoelectric inclusion. The inclusions are polycrystalline $BaTiO_3$. Particularly, their electromechanical coefficients that include the elastic coefficients, piezoelectric and flexoelectric coefficients are a function of the orientation of the crystallites within the polycrystal aggregate. Assuming a Gaussian fiber texture distribution aligned with the polarization direction, the orientation can be quantified to a first approximation through an orientation distribution parameter σ_θ, which denotes the standard deviation of the distribution of θ, the angle of the crystallite with the fiber direction (see Appendix A1). In this way, $\sigma_\theta \to 0$ corresponds to a perfectly oriented condition and $\sigma_\theta \to \infty$ corresponds to randomly oriented configuration. Our model estimates the effective properties of the polycrystalline inclusions by means of volume averaging [30] through the generalized spherical harmonic method [29]. The orientation dependent electroelastic parameters are shown in Fig. 2. These are the effective elastic coefficients, the effective linear piezoelectric coefficients, and the effective electric permittivities for tetragonal crystallites with properties taken from Ref. [30]. Our studies are conducted with $\sigma_\theta = 5.0$ which reasonably corresponds to a random polycrystalline behaviour.

We next describe orientation-dependent flexoelectric coefficients. We assume cubic crystallites since the flexoelectric properties for $BaTiO_3$ are available in the literature only for its cubic piezoelectric phase. It is observed that the shear coefficient of the crystal is difficult to characterize. To study its effect on the behaviour of the composite, and after revisiting the isotropic condition [36], we propose to define a flexoelectric anisotropy factor given by

$$A_f = \frac{2\mu_S}{\mu_L - \mu_T}, \tag{8}$$

where μ_S, μ_L, and μ_T are the shear, longitudinal, and transverse flexoelectric coefficients of $BaTiO_3$ crystals. In such a way that $A_f = 1$ means that the crystal is isotropic. The index A_f quantifies the degree of

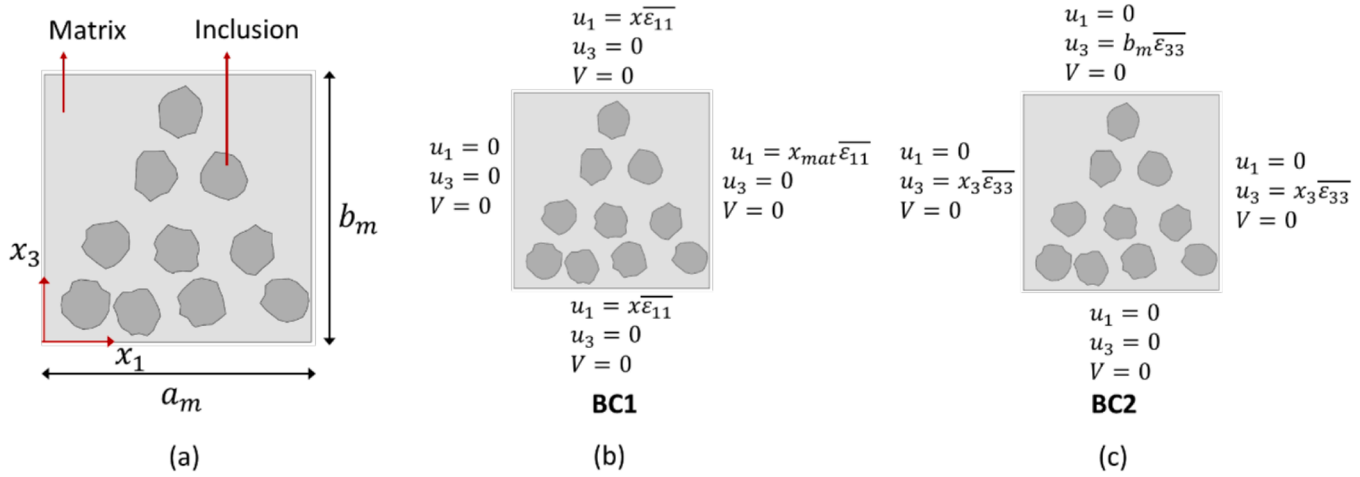

Fig. 1. (a) Representative illustration of a unit cell of a lead-free piezocomposite having a matrix in which piezoelectric inclusions are dispersed, (b) and (c) illustrate the boundary conditions imposed on the displacement components u_1 and u_3, and the electric potential V to compute the effective piezoelectric coefficients e_{31} and e_{33}, respectively. $\overline{\varepsilon_{11}}$ and $\overline{\varepsilon_{33}}$ are boundary strains which are set to small values of 1×10^{-6}.

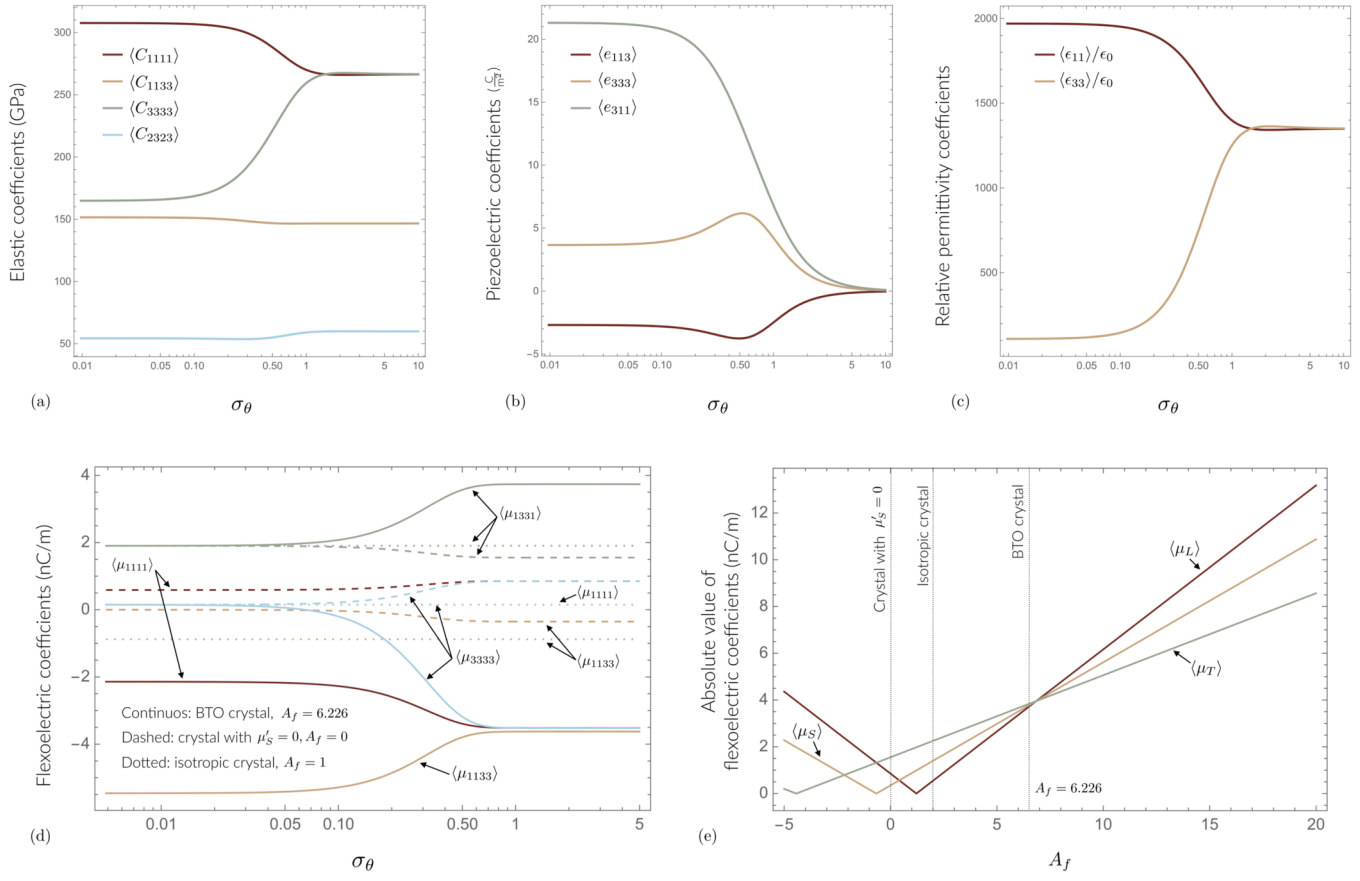

Fig. 2. (a)-(c) Orientation-dependent linear electromechanical coefficients of $BaTiO_3$, (d) Orientation dependent flexoelectric coefficients of $BaTiO_3$, (e) Flexoelectric anisotropy-dependent flexoelectric coefficients of polycrystalline $BaTiO_3$ for a polycrystal with $\sigma_\theta = 5.0$.

flexoelectric anisotropy in cubic crystals. Since the shear coefficient is not well characterized experimentally, theoretical analyses typically assume $\mu_S = 0$ (i.e. $A_f = 0$). However, this is not generally the case as reference [11] theoretically predicts an anisotropic index $A_f = 6.226$. Therefore, we study the effect of the anisotropy parameter to understand what significance it holds in terms of flexoelectric contribution. The dependence of the flexoelectric coefficients of a $BaTiO_3$ polycrystal as a function of σ_θ are shown in Figure 2(d) for different A_f.In Figure 2(e), we show the flexoelectric coefficients as a function of the flexoelectric anisotropy A_f for an orientation parameter $\sigma_\theta = 5$ which is representative of a randomly oriented $BaTiO_3$ crystal inclusion. The detailed derivations of the orientation-dependent flexoelectric coefficients are presented in Appendix A1.

The Young's modulus of the matrices is assumed to be 10^6 Pa which is representative of soft matrices (such a hydrogels) which are highly conducive to flexoelectric effective given the large elastic gradients at

their interface with rigid inclusions. We explore three different forms of matrix behaviour given by three different Poisson's ratios: $\nu_m = -1$ (auxetic), $\nu_m = 0.33$(typicalpolymers), and $\nu_m = 0.499$(incompressible) to understand how the properties of the matrix influence the flexoelectric behaviour of the composite. The elastic coefficients are obtained using the Lame's constants, $\lambda_m = \frac{E_m \nu_m}{(1+\nu_m)(1-2\nu_m)}$, $\mu_m = \frac{E_m}{2(1+\nu_m)}$, as $C_{1111} = C_{3333} = \lambda_m + 2\mu_m, c_{1313} = \lambda_m$,and $c_{2323} = \mu_m$.

Finally, the current study neglects the effects of electrostriction.

3. Results and discussion

The results we present in this section are focused on developing an understanding of two key aspects. Firstly, in Section 3.1, we try to find out how important it is to reconcile the three-orders of magnitude difference between theoretical predictions and experimental measurements of flexoelectric coefficients of $BaTiO_3$. Secondly, in Section 3.2, we try to investigate the need to characterize the shear flexoelectric coefficient experimentally by studying its influence on the flexoelectric coefficients of a lead-free composite. In both experiments, as we would notice, there is a pressing need to fill these gaps in our understanding of flexoelectric properties of lead-free piezocomposites.

3.1. The influence of the flexoelectric scaling factor on the flexoelectric contribution

There is a well-documented order-of-magnitude discrepancy between theoretically estimated and experimentally measured flexoelectric coefficients. As Wang et al. [31] comprehensively discuss, experimental measurements of flexoelectric coefficients in the paraelectric phase of many perovskite oxides reach up to several tens of μC/m, whereas theoretical estimations suggest intrinsic flexoelectricity should not exceed several nC/m. Wang et al. [31] provide a detailed analysis of potential factors contributing to this disparity, which is summarized in their Table 5.3 (not reproduced here), including extrinsic contributions, surface effects, and theoretical calculation ambiguities. Other studies have proposed additional explanations, such as the contribution of dynamic flexoelectricity to the giant static flexoelectric effect in spatially inhomogeneous samples [32], including soft electrets [33], and apparent flexoelectricity due to heterogeneous piezoelectricity [34].

To account for this discrepancy in our study, we introduce a flexoelectric scaling factor S_f. We uniquely define S_f as a multiplicative factor applied to the theoretically predicted flexoelectric coefficients to span the range between theoretical predictions and experimental observations. Mathematically, this can be expressed as:

$$\mu_{\text{eff}} = S_f \, \mu_{\text{th}},$$

where μ_{eff} is the effective flexoelectric coefficient used in our calculations, μ_{th} is the theoretically predicted flexoelectric coefficient, and S_f is our scaling factor. Experimentally measured values of the flexoelectric coefficients of $BaTiO_3$ are around three orders of magnitude higher than the theoretically predicted values [11]. We, accordingly, set $S_f = 1$ and 1000 to study the flexoelectric enhancements in a $BaTiO_3$-based piezocomposite architecture, where $S_f = 1$ corresponds to the theoretically predicted values found in reference [11], and $S_f = 1000$ corresponds to flexoelectric coefficients in reference [11] scaled by a factor of 1000. This approach allows us to study the impact of this theoretical-experimental discrepancy on the flexoelectric behavior of our composite structure.

The normalized e_{31} coefficients, in the case of $S_f = 1$ and 1000, are shown in Fig. 3(a)-(c) for $\nu_m = -0.99$, 0.33, and 0.499, respectively. Similarly, Figure 3(d)-(f) show the corresponding values for the normalized e_{33} coefficients. The normalization is carried out relative to the actual piezoelectric coefficient values for $N = 5$, which represents a size-scale with negligible flexoelectric contribution. The first main observation is that matrices with $\nu_m = 0.33$show the maximum flexoelectric influence among matrices with the three values of ν_m considered here. This class of matrices shows almost an order of magnitude larger flexoelectric contribution than the matrices with $\nu_m = -0.99$ and 0.499, respectively. However, the sign of the flexoelectric enhancement with respect to the direction of the linear flexoelectric coefficient is not straightforward. When we consider theoretical values of the

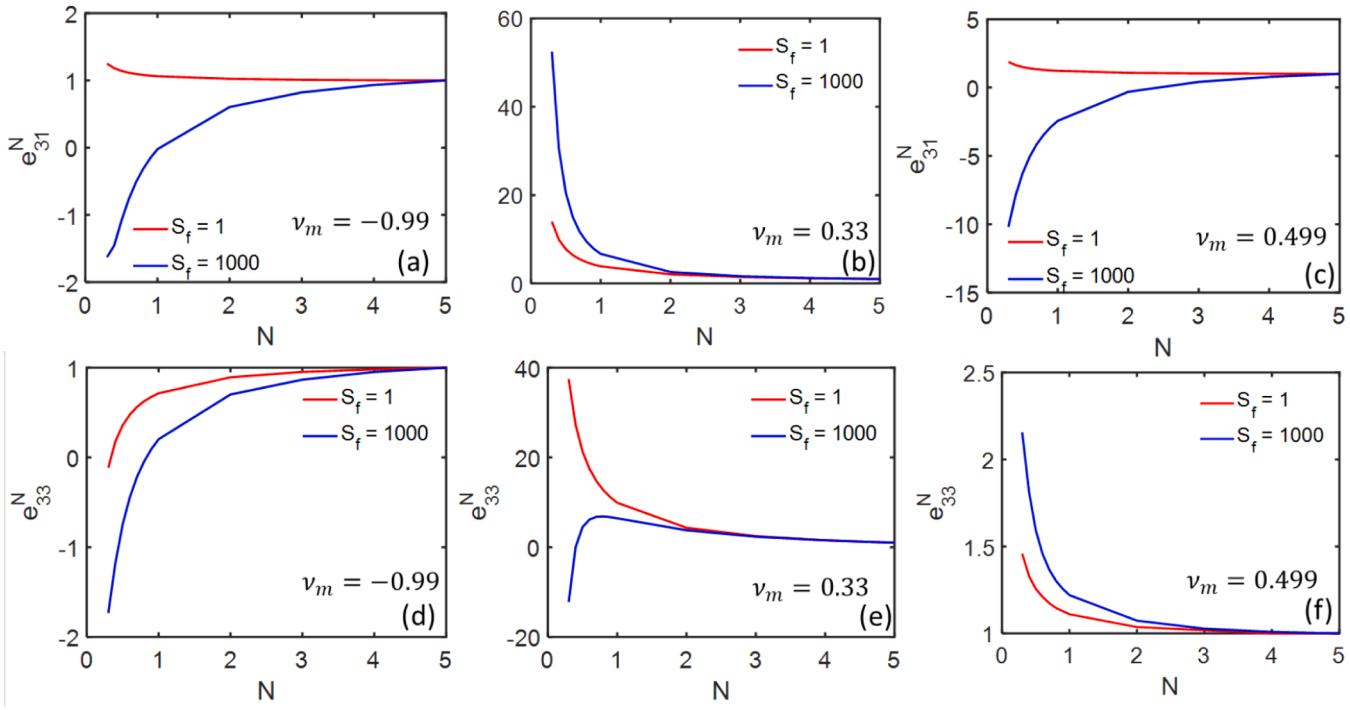

Fig. 3. Variation of normalized e_{31} ((a)-(c)) and normalized e_{33} ((d)-(f)) as a function of the size scale factor, S_f, of the flexoelectric RVE for different Poisson's ratio ν_m of the matrix.

flexoelectric coefficients (i.e. $S_f = 1$) as predicted in reference [11], we see that the flexoelectric contribution reinforces the linear piezoelectric response for both $e_{31}$and e_{33}. When we consider experimental correction to the values ($S_f = 1000$), we notice that the flexoelectric contribution in the case of e_{31} and e_{33} are in the opposite directions. In the case of e_{31},we notice an enhancement by a factor of around 50 due to the reinforcing nature of the flexoelectric contribution. However, in the case of e_{33}, although the flexoelectric contribution reinforces the linear piezoelectric response for larger values of N, at smaller size-scales, the flexoelectric response is large but opposite in direction to the linear piezoelectric response. This change of sign in the properties means that, for some size parameter N, the piezoelectric properties become zero. This suggests that a proper understanding of the factors underlying the discrepancies between the theoretical and practical flexoelectric coefficient values is required for the reliable design of flexoelectric composites.

The change in the sign of the flexoelectric contribution across $S_f = 1$ and $S_f = 1000$ is noticed in a few more cases (Fig. 3(a) and (c)).

3.2. The influence of the flexoelectric anisotropy factor on the flexoelectric contribution

Here, we study the influence of the flexoelectric anisotropy A_f on the flexoelectric contribution for different matrices. All the analyses are carried out with experimental correction to the flexoelectric coefficients (i.e. $S_f = 1000$). The flexoelectric anisotropy factor, as discussed in Section 2.3, is given by $A_f = \frac{2\,\mu_S}{\mu_L - \mu_T}$.

We investigate the cases of $A_f = 0$ (anisotropy, $\mu_S = 0$), $A_f = 1$ (isotropy, $\mu_S = \frac{1}{2}(\mu_L - \mu_T)$), and $A_f = 6.226$ (theoretically predicted value [11]). In almost all the cases of ν_m, we notice from the results in Fig. 4. In all the cases, we notice that the theoretically predicted anisotropy shows a significantly larger flexoelectric contribution compared to the cases with $A_f = 0$ and 1. Notably, in the case of the composite architecture with $\nu_m = 0.33$, we notice that $A_f = 6.226$ results in almost a 2.5-times increase in the e_{31} coefficient with respect to the isotropic and anisotropic cases (at $N = 0.5$). We also notice that in several cases (Fig. 4(a), (c), and (e)), the flexoelectric contribution changes signs as A_f increases.

In summary, these results clearly point out that the shear flexoelectric coefficient, which has been poorly characterized by experiments at this point, has a significant influence on the flexoelectric behaviour of a composite. This suggests that it would be fruitful to direct experimental efforts towards characterizing the shear flexoelectric coefficients. This would help build more reliable size-dependent piezoelectric material models using which advanced lead-free composites and functional devices with tailored electromechanical properties can be designed.

4. Conclusions

Using advanced flexoelectric composite models, we have addressed pertinent questions in flexoelectric composite design stemming from three key issues: the poorly characterized shear flexoelectric coefficient, the significant discrepancies between theoretical predictions and experimental measurements of flexoelectric coefficients, and the poorly understood influence of matrix mechanical properties on flexoelectric behavior. Our parametric flexoelectric model of a lead-free piezocomposite with graded inclusion concentration has provided valuable insights into these issues.

We first note the need to develop a proper understanding of the factors causing almost a 3-fold discrepancy in the flexoelectric coefficients predicted by theory and observed in experiments, as this discrepancy can result in a significant change in the magnitude and direction of the flexoelectric contribution. Further, the study on flexoelectric anisotropy clearly shows that the flexoelectric shear effect and its contributions to the electromechanical properties of lead-free piezocomposites cannot be neglected. Our analysis of matrix properties reveals their substantial influence on the overall flexoelectric behavior of the composite, particularly for matrices with a common Poisson's ratio of 0.33.

While our study focuses on these specific aspects, it is important to acknowledge that the complex nature of flexoelectric phenomena may involve additional factors. Our work underscores the necessity for

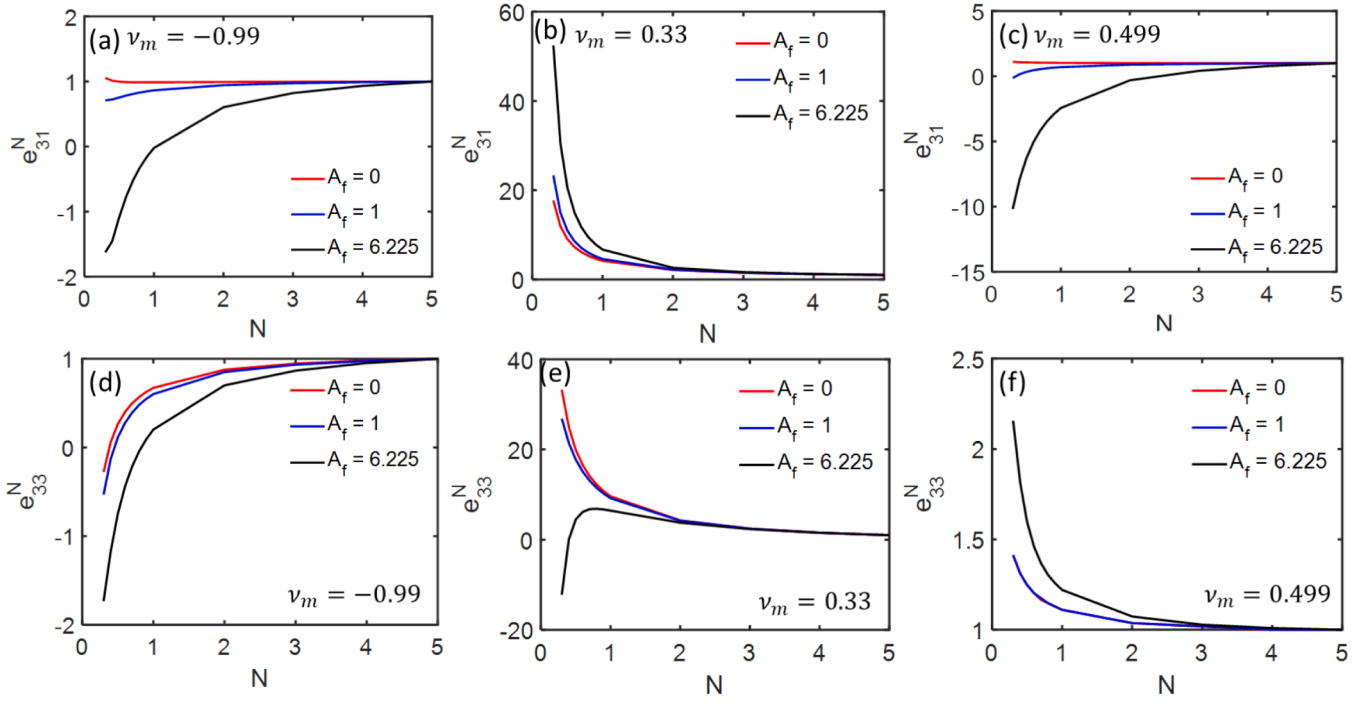

Fig. 4. Variation of normalized e_{31} ((a)-(c)) and normalized e_{33} ((d)-(f)) as a function of the flexoelectric anisotropy factor, A_f, of the $BaTiO_3$ inclusions. The analyses are done for different Poisson's ratios ν_m of the matrix as indicated in the subfigures.

refined models and further experimental studies to build more accurate representations of flexoelectric behavior in composites. These advancements will be crucial for designing tailored composites and devices for different applications based on lead-free materials, where the interplay between various electromechanical effects can significantly influence overall performance.

CRediT authorship contribution statement

A.K. Jagdish: Visualization, Validation, Software, Methodology, Investigation. **Federico C. Buroni:** Writing – review & editing, Writing – original draft, Visualization, Validation, Software, Resources, Project administration, Methodology, Investigation, Funding acquisition, Formal analysis. **Roderick Melnik:** Software, Writing – review & editing, Writing – original draft, Validation, Methodology, Investigation, Formal analysis, Conceptualization. **Luis Rodriguez-Tembleque:** Resources, Investigation, Funding acquisition. **Andrés Sáez:** Resources, Investigation.

Declaration of competing interest

The authors declare that they have no known competing financial interests or personal relationships that could have appeared to influence the work reported in this paper.

Data availability

Data will be made available on request.

Funding

This publication is part of the R+D+i project, PID2022-137903OB-I00, funded by MI- CIU/AEI/10.13039/501100011033/ and by ERDF/EU. R.M. is acknowledging support of NSERC and CRC Program.

Data availability statement

Data can be made available on request to the corresponding author.

Appendix A1

We derive here the orientation-dependent flexoelectric coefficients of polycrystalline $BaTiO_3$.

Let us consider the flexoelectric constitutive law [31]:

$$P_i = \mu_{ijkl}\frac{\partial \varepsilon_{jk}}{\partial x_l} \tag{AE1}$$

where μ_{ijkl} are the components of the fourth-order direct flexoelectric tensor, satisfying the symmetries $\mu_{ijkl} = \mu_{ikjl}$. These components relate the electric polarization vector $\boldsymbol{P}$ to the gradient of the strain tensor $\boldsymbol{\varepsilon}$, under the assumption of small deformations.

This work focuses on crystalline aggregates with a fiber texture distribution of crystallites and formed by crystals with cubic symmetry. Specifically, we consider a Gaussian texture with the orientation distribution function (ODF) given by

$$w(\theta, \sigma_\theta) = \frac{\exp\left(-\dfrac{\theta^2}{2\sigma_\theta^2}\right)}{\sqrt{2\pi}\sigma_\theta}, \tag{AE2}$$

where θ represents the Euler angle relative to the x_3 axis, and σ_θ is the standard deviation of this Gaussian distribution. Note that this Gaussian ODF is independent of the other two Euler angles, ψ and θ.

The direct flexoelectric tensor $\boldsymbol{\mu}'$ for cubic materials referred to a principal material system $x_i'(i = 1\ldots3)$ has 3 independent coefficients satisfying [35]

$$\begin{aligned} \mu'_{1111} &= \mu'_{2222} = \mu'_{3333} = \mu'_L, \\ \mu'_{1122} = \mu'_{1133} &= \mu'_{2121} = \mu'_{2233} = \mu'_{3131} = \mu'_{3232} = \mu'_S, \\ \mu'_{1221} = \mu'_{1331} &= \mu'_{2332} = \mu'_{3113} = \mu'_{3223} = \mu'_T, \end{aligned} \tag{AE3}$$

with all other coefficients being zero. Coefficients μ'_L, μ'_S, and μ'_T are usually called longitudinal, shear, and transverse coefficients, respectively.

When a cubic crystal is oriented statistically as described by the ODF (AE2), the effective or macroscopic flexoelectric behaviour $\boldsymbol{\mu}$ assumes a matrix structure indicative of transversely isotropic behaviour, as elucidated by Buroni et al. [36]. Consequently, for a polycrystal with such effective symmetry and under the assumption of plane strain in the $x_1 - x_3$ plane (i.e., $\varepsilon_{12,2} = \varepsilon_{22,1} = \varepsilon_{23,2} = \varepsilon_{22,3} = 0$), the constitutive law (AE1) reduces to

$$P_1 = \mu_{1111}\varepsilon_{11,1} + 2\mu_{1133}\varepsilon_{13,3} + \mu_{1331}\varepsilon_{33,1}, \tag{AE4}$$

and

$$P_3 = \mu_{1331}\varepsilon_{11,3} + 2\mu_{1133}\varepsilon_{13,1} + \mu_{3333}\varepsilon_{33,3}, \tag{AE5}$$

with the comma denoting differentiation. Therefore, we need to account for the coefficients μ_{1111}, μ_{1133}, μ_{3311}, and μ_{3333} of the polycrystal.

Following the model proposed by Buroni et al., [36], the effective flexoelectric tensor is estimated through the orientation average of the crystal's flexoelectric properties, weighted by the ODF. This is expressed as:

$$\boldsymbol{\mu} = 8\pi^2 \int_{SO(3)} \boldsymbol{\mu}'(\psi,\ \theta, \phi) w(\psi,\ \theta, \phi) dg, \tag{AE6}$$

where dgrepresents the Haar measure on the $SO(3)$, with $8\pi^2 dg = d\mathscr{V}$ and $\mathscr{V}$ denoting the volume measure of $SO(3)$. The ODF satisfies the normalization condition $\int_{SO(3)} w d\mathscr{V} = 1$. Buroni et al. provide closed-form expressions for these averages in terms of the texture coefficients [36]. When the ODF, w, is specified by the fiber texture (AE2), the necessary expressions for computing the plane strain constitutive laws (AE4) and (AE5) are

$$\begin{aligned}
\mu_{1111} &= \frac{1}{15}\left(3\mu_B - 2\pi^2 c_{00}^4 \mu_A\right)\\
\mu_{1133} &= \frac{1}{45}\left(8\pi^2 c_{00}^4 \mu_A - 9\mu_C\right),\\
\mu_{1331} &= \frac{1}{45}\left(8\pi^2 c_{00}^4 \mu_A + 9(\mu_B + 2\mu_C)\right),\\
\mu_{3333} &= \frac{1}{45}\left(9\mu_B - 16\pi^2 c_{00}^4 \mu_A\right),
\end{aligned} \tag{AE7}$$

where $\mu_A = \mu'_T + 2\mu'_S - \mu'_L$, $\mu_B = 2\mu'_T + 4\mu'_S + 3\mu'_L$, and $\mu_C = \mu'_T - 3\mu'_S - \mu'_L$. Texture is accounted for through the texture coefficient c_{00}^4. An analytical expression for this coefficient as a function of the standard deviation σ_θ and its formal definition are provided in Ref. [36].

In order to study the impact of the shear flexoelectric coefficient of the crystal on the overall behaviour, we propose the following flexoelectric anisotropy index [36]

$$A_f := \frac{2\mu'_S}{\mu'_L - \mu'_T} \tag{AE8}$$

where $A_f = 1$ implies isotropic material behaviour, while when $A_f = 0$ the shear coefficient μ'_S is zero. This index quantifies the degree of flexoelectric anisotropy in cubic materials. The coefficients μ'_L and μ'_T for the crystal are sourced from Maranganti and Sharma [11] (refer to Table AT1). The shear flexoelectric coefficient is then defined as $\mu'_S = A_f \frac{\mu'_L - \mu'_T}{2}$. For the BTO crystal, as calculated by Maranganti and Sharma [11], the value of the flexoelectric anisotropy index is $A_f \approx 6.226$.

Table AT1
Flexoelectric coefficients for cubic crystal properties of BTO computed by lattice dynamics approach (LDA) method [11].

Estimation method	μ'_L(nC/m)	μ'_T(nC/m)	μ'_S(nC/m)
LDA [11]	0.15	1.904	−5.46

Fig. AF1 shows the variation of the effective values of the flexoelectric coefficients μ_{1111},μ_{1133},μ_{1331}, and μ_{3333} as a function of the standard deviation σ_θ for different anisotropy indices A_f. Continuous lines correspond to the estimations when the properties of the crystal are sourced from Maranganti and Sharma [11]; here, the anisotropy index is $A_f = 6.226$. Dashed lines represent the effective estimations obtained when the shear coefficient of the crystal is forced to be zero, i.e. $A_f = 0$. It is observed that the influence of the dispersion, σ_θ, on the effective properties is marginal compared to the former example. Lastly, dotted lines describe the behaviour when the crystal is considered isotropic, i.e. $A_f = 1$. As expected, no variation in the effective properties is observed. Moreover, in this case, $\mu_{1111} = \mu_{3333}$.

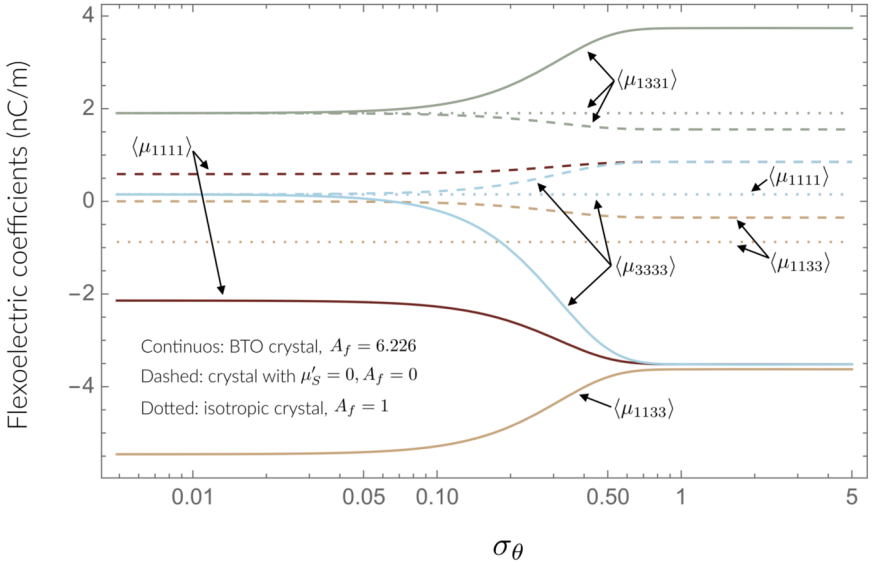

Fig. AF1. Effective μ_{1111},μ_{1133},μ_{1331},andμ_{3333} as a function of the standard deviation σ_θ for different anisotropic indices A_f.

References

[1] T.D. Nguyen, S. Mao, Y. Yeh, P.K. Purohit, M.C. McAlpine, Nanoscale flexoelectricity, Adv. Mater. 25 (7) (Feb. 2013) 946–974, https://doi.org/10.1002/adma.201203852.

[2] P.V. Yudin, A.K. Tagantsev, Fundamentals of flexoelectricity in solids, Nanotechnology 24 (43) (Nov. 2013) 432001, https://doi.org/10.1088/0957-4484/24/43/432001.

[3] A. Abdollahi, D. Millán, C. Peco, M. Arroyo, I. Arias, Revisiting pyramid compression to quantify flexoelectricity: a three-dimensional simulation study, Phys. Rev. B 91 (10) (Mar. 2015) 104103, https://doi.org/10.1103/PhysRevB.91.104103.

[4] A. Abdollahi, N. Domingo, I. Arias, G. Catalan, Converse flexoelectricity yields large piezoresponse force microscopy signals in non-piezoelectric materials, Nat. Commun. 10 (1) (Mar. 2019) 1266, https://doi.org/10.1038/s41467-019-09266-y.

[5] J.A. Krishnaswamy, F.C. Buroni, R. Melnik, L. Rodriguez-Tembleque, A. Saez, Advanced modeling of lead-free piezocomposites: the role of nonlocal and nonlinear effects, Compos. Struct. 238 (Apr. 2020) 111967, https://doi.org/10.1016/j.compstruct.2020.111967.

[6] J.A. Krishnaswamy, L. Rodriguez-Tembleque, R. Melnik, F.C. Buroni, A. Saez, Size dependent electro-elastic enhancement in geometrically anisotropic lead-free piezocomposites, Int. J. Mech. Sci. 182 (Sep. 2020) 105745, https://doi.org/10.1016/j.ijmecsci.2020.105745.

[7] J.A. Krishnaswamy, F.C. Buroni, R. Melnik, L. Rodriguez-Tembleque, A. Saez, Flexoelectric enhancement in lead-free piezocomposites with graded inclusion concentrations and porous matrices, Comput. Struct. 289 (Dec. 2023) 107176, https://doi.org/10.1016/j.compstruc.2023.107176.

[8] P.K. Panda, Review: environmental friendly lead-free piezoelectric materials, J. Mater. Sci. 44 (19) (Oct. 2009) 5049–5062, https://doi.org/10.1007/s10853-009-3643-0.

[9] Y. Saito, et al., Lead-free piezoceramics, Nature 432 (7013) (Nov. 2004) 84–87, https://doi.org/10.1038/nature03028.

[10] S. Cho, et al., Switchable tribology of ferroelectrics, Nat. Commun. 15 (1) (Jan. 2024) 387, https://doi.org/10.1038/s41467-023-44346-0.

[11] R. Maranganti, P. Sharma, Atomistic determination of flexoelectric properties of crystalline dielectrics, Phys. Rev. B 80 (5) (Aug. 2009) 054109, https://doi.org/10.1103/PhysRevB.80.054109.

[12] A. Abdollahi, C. Peco, D. Millán, M. Arroyo, I. Arias, Computational evaluation of the flexoelectric effect in dielectric solids, J. Appl. Phys. 116 (9) (Sep. 2014), https://doi.org/10.1063/1.4893974.

[13] Alice Mocci, Computational Modeling and Rational Design of Flexoelectric Metamaterials and Devices, Universitat Politècnica de Catalunya, 2021, https://doi.org/10.5821/dissertation-2117-351105.

[14] M. Bahrami-Samani, S.R. Patil, R. Melnik, Higher-order nonlinear electromechanical effects in wurtzite GaN/AlN quantum dots, J. Phys. Condens. Matter 22 (49) (Dec. 2010) 495301, https://doi.org/10.1088/0953-8984/22/49/495301.

[15] B. He, B. Javvaji, X. Zhuang, Characterizing flexoelectricity in composite material using the element-free galerkin method, Energies (Basel) 12 (2) (Jan. 2019) 271, https://doi.org/10.3390/en12020271.

[16] Z. Kuang, Internal energy variational principles and governing equations in electroelastic analysis, Int. J. Solids Struct. 46 (3–4) (Feb. 2009) 902–911, https://doi.org/10.1016/j.ijsolstr.2008.10.001.

[17] R.L. Goldberg, M.J. Jurgens, D.M. Mills, C.S. Henriquez, D. Vaughan, S.W. Smith, Modeling of piezoelectric multilayer ceramics using finite element analysis, IEEE Trans. Ultrason. Ferroelectr. Freq. Control 44 (6) (Nov. 1997) 1204–1214, https://doi.org/10.1109/58.656622.

[18] S.Y. Wang, A finite element model for the static and dynamic analysis of a piezoelectric bimorph, Int. J. Solids Struct. 41 (15) (Jul. 2004) 4075–4096, https://doi.org/10.1016/j.ijsolstr.2004.02.058.

[19] Z. Lašová, R. Zemčík, Comparison of finite element models for piezoelectric materials, Procedia Eng 48 (2012) 375–380, https://doi.org/10.1016/j.proeng.2012.09.528.

[20] X. Tian, et al., Analytical studies on mode III fracture in flexoelectric solids, J. Appl. Mech. 89 (4) (Apr. 2022), https://doi.org/10.1115/1.4053268.

[21] T. Profant, J. Sládek, V. Sládek, M. Kotoul, Assessment of amplitude factors of asymptotic expansion at crack tip in flexoelectric solid under mode I and II loadings, Int. J. Solids Struct. 269 (May 2023) 112194, https://doi.org/10.1016/j.ijsolstr.2023.112194.

[22] X. Tian, J. Sladek, V. Sladek, Q. Deng, Q. Li, A collocation mixed finite element method for the analysis of flexoelectric solids, Int. J. Solids Struct. 217–218 (May 2021) 27–39, https://doi.org/10.1016/j.ijsolstr.2021.01.031.

[23] J. Sladek, V. Sladek, S.M. Hosseini, Analysis of a curved Timoshenko nano-beam with flexoelectricity, Acta Mech. 232 (4) (Apr. 2021) 1563–1581, https://doi.org/10.1007/s00707-020-02901-6.

[24] R. Maranganti, P. Sharma, Length scales at which classical elasticity breaks down for various materials, Phys. Rev. Lett. 98 (19) (May 2007) 195504, https://doi.org/10.1103/PhysRevLett.98.195504.

[25] N.D. Sharma, R. Maranganti, P. Sharma, On the possibility of piezoelectric nanocomposites without using piezoelectric materials, J. Mech. Phys. Solids 55 (11) (Nov. 2007) 2328–2350, https://doi.org/10.1016/j.jmps.2007.03.016.

[26] K. Tannhäuser, P.H. Serrao, S. Kozinov, Second-order collocation-based mixed FEM for flexoelectric solids, Solids 4 (1) (Feb. 2023) 39–70, https://doi.org/10.3390/solids4010004.

[27] A. Froehlich, A. Brueckner-Foit, and S. Weyer, "Effective properties of piezoelectric polycrystals," Jun. 2000, pp. 279–287. doi: 10.1117/12.388212.

[28] A.A. Saputra, V. Sladek, J. Sladek, C. Song, Micromechanics determination of effective material coefficients of cement-based piezoelectric ceramic composites, J. Intell. Mater. Syst. Struct. 29 (5) (Mar. 2018) 845–862, https://doi.org/10.1177/1045389X17721047.

[29] J.L. Buroni, F.C. Buroni, Averaging material tensors of any rank in textured polycrystalline materials: extending the scope beyond crystallographic proper point groups, Int. J. Eng. Sci. 193 (Dec. 2023) 103942, https://doi.org/10.1016/j.ijengsci.2023.103942.

[30] J.Y. Li, The effective electroelastic moduli of textured piezoelectric polycrystalline aggregates, J. Mech. Phys. Solids 48 (3) (Mar. 2000) 529–552, https://doi.org/10.1016/S0022-5096(99)00042-3.

[31] B. Wang, Y. Gu, S. Zhang, L.-Q. Chen, Flexoelectricity in solids: progress, challenges, and perspectives, Prog. Mater Sci. 106 (Dec. 2019) 100570, https://doi.org/10.1016/j.pmatsci.2019.05.003.

[32] A.N. Morozovska, E.A. Eliseev, Size effect of soft phonon dispersion in nanosized ferroics, Phys. Rev. B 99 (2019) 115412, https://doi.org/10.1103/physrevb.99.115412.

[33] A.H. Rahmati, S. Bauer, P. Sharma, S. Yang, S. Bauer, P. Sharma, et al., Nonlinear bending deformation of soft electrets and prospects for engineering flexoelectricity and transverse d31 piezoelectricity, Soft Matter 15 (2019) 127–148, https://doi.org/10.1039/c8sm01664j.

[34] J. Yvonnet, X. Chen, P. Sharma, Apparent flexoelectricity due to heterogeneous piezoelectricity, J. Appl. Mech. 87 (11) (2020) 111003.

[35] L. Shu, X. Wei, T. Pang, X. Yao, C. Wang, Symmetry of flexoelectric coefficients in crystalline medium, J. Appl. Phys. 110 (10) (Nov. 2011), https://doi.org/10.1063/1.3662196.

[36] J.L. Buroni, R. Melnik, L. Rodríguez-Tembleque, A. Sáez, F.C. Buroni, Closed-form expressions for computing flexoelectric coefficients in textured polycrystalline dielectrics, Appl. Math. Model 125 (Jan. 2024) 375–389, https://doi.org/10.1016/j.apm.2023.09.032.